Journal of Research in Medical and Dental Science
2018, Volume 6, Issue 4, Page No: 36-41

Available Online at: www.jrmds.in
eISSN No. 2347-2367: pISSN No. 2347-2545

A Novel Method for Noticing Dental Infections by Means of Rapid Synthetic Nervous System

Adnan Mahmood*

Department of Basic Sciences, College of Dentistry, University of Baghdad, Iraq

ABSTRACT

Aim of the study: This study aimed to use a statistical method to treat the images enhance the periodontist oral treatment, the idea is to use couple graphs for inspection which lead to outcome background differences.
Materials and Methods: A new procedure was adopted depends on performance of irritated linking in the incidence of area between the image and the mass of Rapid Nervous System (RNS). The numerical image deduction was applied on nearly each illness procedure which marks dental solid tissues and development affected in analytic act. The collected figures observe the individualities of unique images which were meaningfully improved afterward deduction concerning visual characteristics as clarity, difference, acuity and tenacity.
Results: Equations where developed and derived (14 Equations), Figures were collected (6 of them) were to follow the deduction concerning visual characteristics as clarity, difference, acuity and tenacity, while the other three were drawn to compare the gathered data, in addition to the tables that was collect all the measurement, all these figures and tables were the sum of totaling stages vital for the obtainable RNS which was lower than that expected by Traditional Nervous Systems (TNS). Virtual outcomes were hypothetically calculated. Some of the limits of Direct Numerical Radiography (DNR) are din.
Conclusion: A new quick process for dental illnesses recognition was obtained in addition, it reduce the assembly din remains as significant influence in precise analysis of oral pathological lesions.

Key words: Synthetic nervous, Dental infection, Technique

HOW TO CITE THIS ARTICLE: Adnan Mahmood*, A novel method for noticing dental infections by means of rapid synthetic nervous system, J Res Med Dent Sci, 2018, 6 (5):36-41

Corresponding author: Adnan Mahmood
e-mail✉: adnanm2007@yahoo.com
Received: 24/07/2018
Accepted: 06/08/2018

INTRODUCTION

Numerical Deduction Radiography (NDR) is automated picture handling method which indicates a larger analytical assessment in the inspections of mass and numbers of minor periodontal bone wounds than likely radiography [1].

Deduction Radiography (DR) became familiarized with dentistry start from the eighteens of the last century by way of a technique to enable imagining zones being losing or be gained. The usage of statistical images treating methods has enhanced the sympathy of intra-oral radio-graphs aimed at the discovery of small big changes in periodontist [2,3]. The idea fundamental deduction radio-graph is modest. An image dispensation, processor deducts totally the static assemblies usually from a couple of radio-graphs occupied at two unlike inspections (reference and proceeding image), outcome is a neuter grey background in zones that have no different. Conventionally, zones of bone gaining can be noticed in deep grey blacker than the surround and zones of bone damage look brighter. The capability of doctors are to discover tiny changes in bone using deduction radio-graph which verified by a number of researchers using artificially prompted cuts in the skulls [4,5].

Other researches were accomplished by investigational animals. Minor hydroxyl-apatite thin slices (chips) which used onto pretend osseous lesions while the solid lineal connection which observed among the lesions magnitude and the cluster that studied of deduction between radio-graphs and actual size of the chip and cluster. Those earlier studies engaged cranium investigational animals [6].

The study was achieved to find new statistical method to treat the images to improve the periodontist oral treatment, the design of this study was planned to use a couple of graphs for inspection that lead to differences in outcome background.

MATERIALS AND METHODS

Dual dental descriptions involved in our survey. The variation among them f(x, y) and h(x, y) are stated in the below relation:

$$g(x,y) = f(x,y)-h(x,y) \quad (1)$$

where f(x,y) represent the authentic image which has din arrangement, while h(x,y) represent the background of unique image which considered as reference image that has a luminous pixels formed as of unique image, g(x,y) considered as the outcome image which proves changes among unique and background image [7]. The key practicality of deduction is the improvement of changes between images. The most valuable usage to image deduction in the region of medicinal designate called Front Manner Radio-graph (FMR). Incidentally h(x,y), which located in the front, consider as X-ray image of a zone of patient's body which was taken using accurate TV camera replacing X-ray film determined the other side of X-ray exporter. Such technique contains inject a different center of patient's blood flow, takeover a sequence of images related to functional zone depicted in h(x,y), by subtracting this cover from a sequence of received images afterward injection of the different intermediate. The remaining consequence of deducting the cover as of every sample exist among incoming flow of TV pictures stays in the zones which are dissimilar between f(x,y) and h(x,y) that can be noticed in the produced appearance as improved aspect. Since images could be occupied at TV averages, these processes give complete film display by what means the different median spreads via the several blood vessels among the detected zone [8]. Lately, the calculated radio-graph (CR), that offers directly a numerical achievement of X-ray images, was improved and extensively recognized. Regular radio-graphs ensured difficulties in making and transfer images, while the CR method solved part of those limits, though image goodness is lesser than predictable radio-graphs [9]. Numerical deduction radio-graph structure used to be well-known for line up clinically in vivo radio-graphs upon the implements of the automatic symmetrical registering technique and the different alteration method [7].

DEDUCTION APPLICATION

Radiography technique

Numerical image deduction consider as a technique for structure reduction noise of regular anatomic aspect. Thus it raises the sign to noise relation presented in Equation 1. By means of raising the indication to din relation, the pathology must lead to extra obvious to human viewer. Numerical image deduction was applied on nearly each illness procedure which marks dental solid tissues [10]. Development affected in analytic act which obviously verified in frequent studies. A requirement for numerical deduction radiography is that the plans that must be matching or almost matching at the diverse inspections. Other requirements for deduction are the capability to appropriately arrange in a line to the both of them (images), this is referred to registering and capability to precise for differences related with contact and dispensation that would incomprehensible the variations in radio-graphic compactness related to pathology. Requirement has partial through medical use to that method. New progresses in effective radiographic methods and gamma adjustment processes may afford the responses for those restriction. The use of linear radio-graphic evaluation methods like deduction radiography can withhold most potential for refining analytical accurateness. Visual density of radiographs was digitized into dull stages using drum–scanning densitometer together with high accurateness [11]. Numerical deduction radiography needs close identical of the difference within pictures must deduct. Deduction radiography is a possibly great technique for checking the outcomes of periodontal treatment.

The fruitful use to linear revisions needs such a differences produced by uninhibited fluctuations in X-ray imaging geometry, also using film disclosure and treating situations, be minor comparative with fluctuations of analytical notice happening completed the remark intermission. Whereas those previous conditions are hard to achieve, measured revisions have established that geometric processes by means of occlusal patterns outcome in discovery of periodontal injuries which meaningfully enhanced through conservative radiographic means [12].

The film differences reproduction can be upheld using electric controller of contact time, X-ray tube current and voltage wave systems, and using suspicious film treating with quality control of substances. In spite of those hard works, differences make arise in preparation. Mat lab database of deduction radio-graph used to complete the deduction among unique image f(x,y) and background of unique image h(x,y).

The outcomes of the current investigation are displayed in Figures 1-6. Figure 1 expressed supplement to unique image in ''Mat lab approach'', Figure 3 denote the background to unique image, while Figures 2,4 and 6 display the diagrams to unique images, background and ultimate images correspondingly. Figure 5 denotes the ultimate deducted images. These Figures, can observed the individualities of unique images were meaningfully improved afterward deduction concerning visual characteristics as clarity, difference, acuity and tenacity.

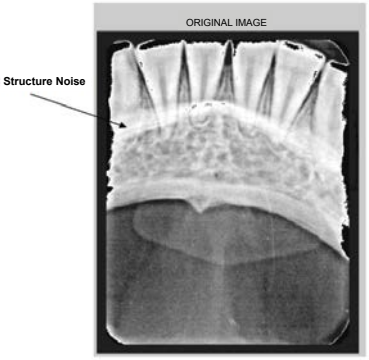

Figure 1: Original image with structure noise

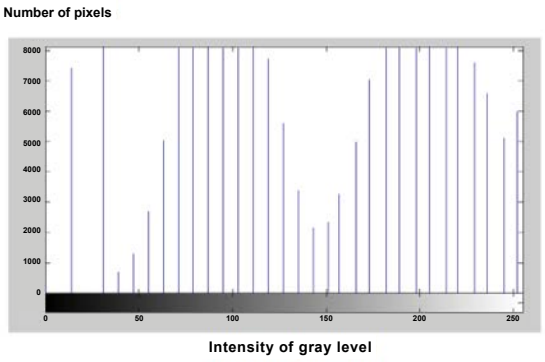

Figure 2: Histogram of the original image

Figure 3: Background of the original image

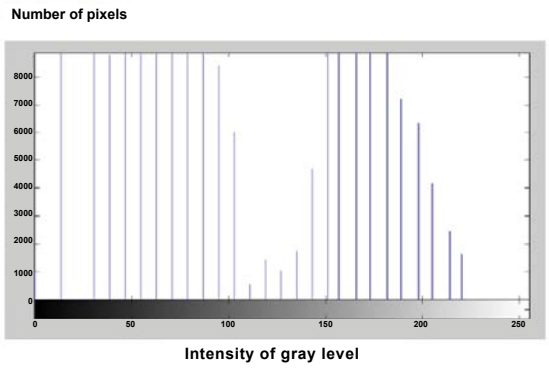

Figure 4: Histogram of the background of the original image

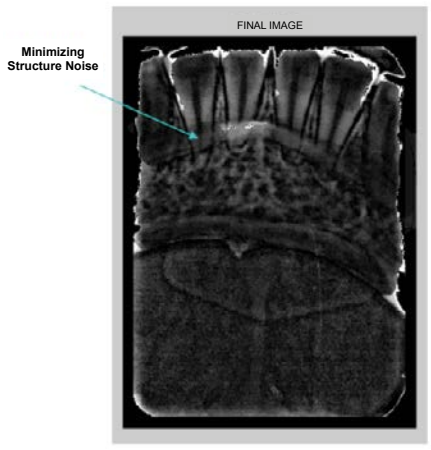

Figure 5: Final image derived from the original image with minimized structure noise

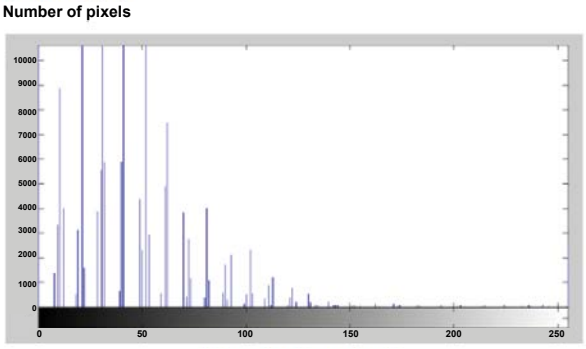

Figure 6: Histogram of the final image

Recognition of primary bone illnesses or initial indirect dental illnesses were main difficulties opposite dentists earlier the start of TNS and NDR. Beforehand DNR, bone annihilation can't notice on the dental radio-graph previously 49%–61% demineralization happens. DNR offers an extremely delicate analytical imaging model which improves exposure of initial bone variations because of high clearness.

The Wild Dental Illnesses Discovery (WDID) were obtained by the means of Neural Systems (NS) in addition to Cross Relationship to Regularity Area (CRRA) by recognition phase, a sub-image X of size mxz (sliding window) can be take out as of the verified image, whose magnitude PxT, which nourished to the neural system. Suppose Wi be weights that has direction (direction quantity) among the input sub-images and the hidden layer. This quantity has a magnitude of mxz and could be signified as mxz matrix. The yield of unknown neurons hi could be determined as follows:

$$hi = g\{\sum_{j=1}^{m}\sum_{k=1}^{z} Wi(j,k)\ x(j,k) + bi\ \} \quad (2)$$

Where, g represents the initiation function and bi represent the partiality of unknown neuron (i). Equation 2 embodies the yield of any unknown neuron to a specific sub-image I. Calculation to the whole image Ψ can be found as follows:

$$hi(uy) = g\{\sum_{j=-\frac{m}{2k}}^{\frac{m}{2}} Wi(j,\ k)\sum_{k=-\frac{z}{2}}^{\frac{z}{2}} Wi(j,\ k)\varphi(u+j, v+k) + bi\ \} \quad (3)$$

Equation (3) embodies a cross connections processes, particularly, every two functions f and g, those functions could be calculated by the following equation [13]:

$$g(x,y)\,x\,f(x,y) = \sum_{m=-\infty}^{\infty}\sum_{z=-\infty}^{\infty} g(m,z)\,f(x+m, y+z) \quad (4)$$

Thus, Equation (3) can be represented in Equation (6) below [14]:

$$h_i = g(W_i x \Psi + b_i) \quad (5)$$

$W_i x\varphi = F^{-1}(F(\Psi)*F^{*(Wi)})$ (6)

The symbol (*) represent the combine in FFT aimed at bulk background. Therefore, by assessing the cross correlate ion, the accelerating ratio can be found analogous to predictable neural systems. Similarly, the last yield of the neural system could be assessed according to the following:

$$O(u,v) = g\{\sum_{i=1}^{q} Wo(i)\,hi(u,v) + bo\} \quad (7)$$

Where, q reflects the sum of neurons inside the unknown film. O(u,v) is neural system productivity while the descending window positioned at (u,v) in the feeding image Ψ. Wo is the mass medium among unknown and yield film.

The difficulty of relationship in the rate area can be evaluated as the following:

1. A verified image of N×N pixels, the 2D-FFT needs a quantity equivalent to $N^2\log_2 N^2$ of compound calculation stages.

2. At every neuron to unknown film, the converse 2DFFT is calculated. So, q retrograde then (1+q) advancing alters must be calculated. Regarding images under exam, the whole amount of the 2D-FFT to compute is $(2q+1)\ N^2\log_2 N^2$.

3. A quantity of multipart calculation stages equivalent to qN^2 must be added.

4. It is recognized that the $(N^2/2)\ \log_2 N^2$ increases and $N^2\log_2 N^2$ additions [15].

5. Any complex growth can be calculated by six real fluctuating point processes and every complex addition is implemented by two real fluctuating point processes. Consequently, the whole amount of calculation stages essential towards finding the 2D-FFT of an N × N image as the following:

$$\rho = 6\left(\left(\frac{N^2}{2}\right)log_2 N^2 + 2\left(N^2 log_2 N^2\right)\right) \quad (8)$$

This may be simplified to: $\rho = 5\ N^2\log_2 N^2$ (9)

Execution multifaceted dot produce in the incidence area also needs $6qN^2$ actual processes.

6. Let's suppose the input needs a scope of (n×n) sizes. And Zeros=(N2-n2) has to be supplementary to the mass medium. Those stages=$q(N^2-n^2)$ are to all neurons. The actual quantity of calculation stages=qN^2 essentially added to find the combined to mass medium for altogether neurons. Also, the amount of actual counting stages equivalent to N essentially to generate nerves multifaceted numbers ($e^{-jk(2\Pi n/N)}$), whereas 0<K<L. Thus, the whole quantity of calculation stages essential to form neural nets converts:

$\sigma = (2q+1)\ (5N^2\log_2 N^2) + 6qN^2 + q(N^2-n^2) + qN^2 + N$ (10)

This can be reformulated as:

$\sigma = (2q+1)(\ 5N^2\log_2 N^2\ ) + q(8N^2 - n^2\ ) + N$ (11)

7. By means of n × n to equal images to N × N pixels, $q(2n^2-1)(N-n+1)^2$ calculation stages remain essential by means of old neural nets to thing finding processes. The theoretic rapidity factor η calculated according to [16]:

$$\eta = \frac{q\left(2n^2-1\right)(N-n+1)^2}{\left(2q+1\right)\left(5N^2 log_2 N^2\right) + q\left(8N^2 - n^2\right) + N} \quad (12)$$

The theoretic speediness in Equation 12 diverse masses to feeding image can be found in Table 1. Applied ratio to operate image of dissimilar size and dissimilar in matrices can be found in Table 2 and by using 2.7 GHz processor and MAT LAB verses 5.3. The consequence of (n) on the quantity of calculation stages is minor and unnoticed. In applied application, the increase procedure used additional time. Below equation (ηm) shows the relationship among the sum of stages essential by FNNs:

$$\eta_m = \frac{qn^2(N-n+1)^2}{\left(2q+1\right)\left(3N^2 log_2 N^2\right) + 6qN^2}$$

Table 1: Practical speed up ratio for images with different sizes using MATLAB Ver. 5.3

Image size	Speed up ratio (n=20)	Speed up ratio (n-25)	Speed up ratio (n=30)
100 × 100	7.88	10.75	14.69
200 × 200	6.21	9.19	13.17
300 × 300	5.54	8.43	12.21
400 × 400	4.78	7.45	11.41
500 × 500	4.68	7.13	10.79
600 × 600	4.46	6.97	10.28
700 × 700	4.34	6.83	9.81
800 × 800	4.27	6.68	9.6
900 × 900	4.31	6.79	9.72
1000 × 1000	4.19	6.59	9.46
1100 × 1100	4.24	6.66	9.62
1200 × 1200	4.2	6.62	9.57
1300 × 1300	4.17	6.57	9.53
1400 × 1400	4.13	6.53	9.49
1500 × 1500	4.1	6.49	9.45
1600 × 1600	4.07	6.45	9.41
1700 × 1700	4.03	6.41	9.37
1800 × 1800	4	6.38	9.32
1900 × 1900	3.97	6.35	9.28
2000 × 2000	3.94	6.31	9.25

Table 2: The theoretical speed up ratio for the images with different sizes

Image size	Speed up ratio (n=20)	Speed up ratio (n-25)	Speed up ratio (n=30)
100 × 100	3.67	5.04	6.34
200 × 200	4.01	5.92	8.05
300 × 300	4	6.03	8.37
400 × 400	3.95	6.01	8.42
500 × 500	3.89	5.95	8.39
600 × 600	3.83	5.88	8.33
700 × 700	3.78	5.82	8.26
800 × 800	3.73	5.76	8.19
900 × 900	3.69	5.7	8.12
1000 × 1000	3.65	5.65	8.05
1100 × 1100	3.62	5.6	7.99
1200 × 1200	3.58	5.55	7.93
1300 × 1300	3.55	5.51	7.93
1400 × 1400	3.53	5.47	7.82
1500 × 1500	3.5	5.43	7.77
1600 × 1600	3.48	5.43	7.72
1700 × 1700	3.45	5.37	7.68
1800 × 1800	3.43	5.34	7.64
1900 × 1900	3.41	5.31	7.6
2000 × 2000	3.4	5.28	7.56

DISCUSSION

Initial nervous systems is qualified for categorize sub-images that enclose illnesses since these that don't and this which can be achieved in the three-dimensional area. In the examination stage, every sub-image within contribution image (experimentally in) is verified from attendance or nonappearance of illnesses. Every pixel location in contribution images and every sub-image increased by a space of substances, that have similar magnitude like sub-image. Such bone increases normally achieved via three-dimensional area. Yield of nervous in the unknown coating were increased by the majorities of the production film.

Ultimately, production in height this explains why the sub-images below exam contains illnesses and vice versa. Consequently, it can be achieved the examining problematic comes across connection to three-dimensional area among the image under exam with contribution weightiness of neural systems.

In present unit, rapid procedure for sensing illnesses was found within dual dimensional irritable associations occurs among the verified image and the sliding window (20 × 20 pixels) is defined. This window was characterized by the neural system bulks located among the contribution item with unknown coating.

Statistical diagrams

The outcomes shown in Figure 7 demonstrate that the outcome of the quantity of growth stages incident to CNNs is higher than FNNs, and for overall relationship, the proportion (η_g) can be redesigned as:

$$\eta_g = \frac{q\left(2n^2-1\right)N^2}{(2Q+1)(5(N+\tau)^2+q(8\left(N+\tau\right)^2-n^2\right)+\left(N+\tau\right)} \quad (14)$$

Whereas Ƭ is a minor quantity, the theoretical proportion relation (η_g) is well-defined in Equation 14 found in Figure 8. Comparing to MAT LAB cross relationship function (XCORR2), experiential outcomes shows that the projected procedure goes rapidly comparing with this function which can be noticed in Figure 9.

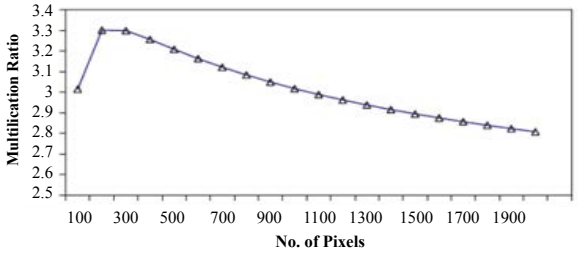

Figure 7: A comparison between the number of multiplication steps for CNNs and FNNs to manipulate images with different sizes (n=20, q-30)

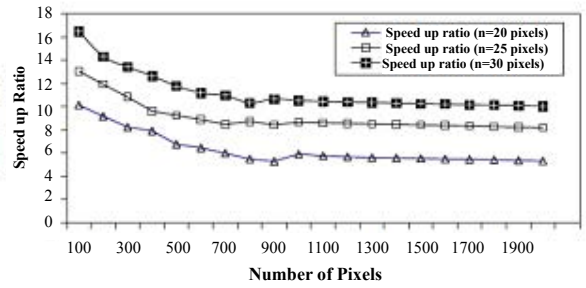

Figure 8: The theoretical speed up ratio for the general faster cross correlation algorithm

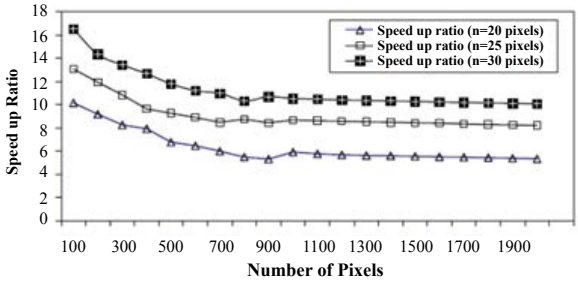

Figure 9: Simulation of the speed up ratio for the general faster cross correlation compared with the MALTAB across correlation function (XCORR3)

The difficulty formula in precise investigation declares a difficulty of (f) with (h) is matching the outcome of the subsequent steps: suppose F and H are outcomes to Fourier change for (f) and (h) inside incidence area. Multiply F and H in the incidence area spot by spot, lately convert the product to three-dimensional area through the opposite Fourier transform [14]. As an outcome, those cross connections could be signified through the product in the incidence area. Therefore, using the cross association inside incidence area rapidity upper in the

sequence of magnitude can be accomplished through the finding procedure [13].

The current study showed that the Numerical Deduction Radiography (NDR) may meaningfully help in the medical analysis of dental infections, when different medical scientific difficulties preventing its general usage overwhelmed. Din in numerical radiography may outcome from foundations other in prognosis geometry through contact. Construction of din contains totally anatomic landscapes except those of analytical attention. Boundaries of basic radiographs in noticing initially, minor jaw cuts are similarly owing to the attendance of assembly din. This work effort is to lower assembly din in numerical dental radiography by means of digital deduction radiography.

This new quick process for dental illnesses recognition was obtained in addition, it reduce the assembly din remains as significant influence in precise analysis of oral pathological lesions.

CONCLUSION

- A new rapid procedure for dental illnesses recognition was obtained.
- This was reached by accomplishment cross connection with frequency area among feeding images and feeding weights of rapid neural systems (FNNs).
- Scientifically, it was approved that the amount of calculating stages essential for the obtainable FNNs is a smaller.
- Imitation outcomes using MAT LAB set the theoretic calculations. Additionally, it was approved that numerical deduction radiography raises analytical accurateness with numeral radiography through noise structure.
- Reducing assembly din remains as significant influence in precise analysis of oral pathological lesions.

REFERENCES

1. Ruttimann UE, Webber RL. Volumetry of localized bone lesions by subtraction n radiography. J Periodontal Res 1987; 22:215-226.
2. Hausmann E, Christersson L, Dunford R, et al. Usefulness of subtraction radiography in the evaluation of periodontal therapy. J Periodontal Res 1985; 1:4-7.
3. Reddy MS, Bruch JM, Jeffcoat MK, et al. Contrast enhancement as an aid to interpretation in digital subtraction radiography. Oral Surg Oral Med Oral Pathol 1991; 71:763–9.
4. Grondahl K, Grodahl H. Influence of variations in projection geometry on the detectability of periodontal bone lesions. J Clin Periodontol 1984; 11:411-20.
5. Bragger D, Pasquali L, Rylander H, et al. Computer–assisted densitometric image analysis in periodontal radiography: A methological study. J Clin Periodontol 1988; 15:27-37.
6. Marjolein H, Anna G, Jan MVD, et al. Preclinical studies and prospective clinical applications for bacteria-targeted imaging: The future is bright. J Clin Transl Imaging 2016; 4:253-64.
7. Jeffcoat MK, Reddy MS, Magnusson L, et al. Efficacy of quantitive digital subtraction radiography using radiographs exposed in Multicenter trial. J Periodontal Res 1996; 31:157–60.
8. Carolina LZV, Bruno C. The history of dentistry and medicine relationship: Could the mouth finally return to the body? J Oral Dis 2009; 15:538-546.
9. Asteria LÁ, Francisco OE, José BM, et al. The application of microencapsulation techniques in the treatment of endodontic and periodontal disease. J Pharm 2011; 3:538–71.
10. Jeffcoat MK, Reddy MS. Digital subtraction radiography for longitudinal assessment of periimplant bone change: Method and validation. Adv Dent Res 1993; 7:196-201.
11. Nakagawa K, Mizuno S, Aoki Y, et al. C-MOS Flat-panel sensor for realtime X-ray imaging. Radiat Med 2000; 18:349-54.
12. Akdeniz BG, Sogur E. An *ex vivo* comparison of conventional and digital radiography for perceived image quality of root fillings. Int Endod J 2005; 38:397-401.
13. Ruttimann E, Richard L, Schmidt E, et al. A robust digital method for film contrast correction in subtraction radiography. J Periodontal Res 1986; 21:486–95.
14. Klette R, Zamperon. Handbook of image processing operators. John Wiley & Sons ltd 1996.
15. Claudiu D, Dritan A, Justin L, et al. Wnt/Beta-catenin signaling reduces central nervous system inflammation in MS. Mult Scler J 2017; 23:2-90.
16. Iyad H, Kershaw AE, Jinous FT, et al. The management of drooling in children and patients with mental and physical disabilities: A literature review. Int J Paediatr Dent 1998; 8:3-11.